DERMATOLOGICA SINICA 33 (2015) 142–145

Contents lists available at ScienceDirect

Dermatologica Sinica

journal homepage: http://www.derm-sinica.com

ORIGINAL ARTICLE

Quantitative assessment of female pattern hair loss

Pei-Kai Hung [1], Thomas Waitao Chu [2, 3], Ren-Yeu Tsai [4], Chien-Wei Kung [1], Sung-Jan Lin [1, 5], Chung-Ming Chen [1, *]

[1] Institute of Biomedical Engineering, National Taiwan University, Taipei, Taiwan
[2] Department of Dermatology, Far Eastern Memorial Hospital, New Taipei City, Taiwan
[3] Oriental Institute of Technology, New Taipei City, Taiwan
[4] Department of Dermatology and Skin Laser Center, Taipei Municipal Wan-Fang Hospital, Taipei Medical University, Taipei, Taiwan
[5] Department of Dermatology, National Taiwan University Hospital and College of Medicine, Taipei, Taiwan

ARTICLE INFO

Article history:
Received: Dec 18, 2013
Revised: Dec 23, 2014
Accepted: Jan 17, 2015

Keywords:
balding width
female pattern hair loss
quantitative analysis

ABSTRACT

Background/Objective: The conventional approach to evaluate female pattern hair loss (FPHL) is to visually inspect and score images of balding area (BA). However, visual estimates vary widely among different physicians, and may hinder objective assessment of hair loss and subsequent treatment response. For this reason, we propose a quantitative method using a computer-aided imaging system to help physicians evaluate the severity of FPHL clinically.
Methods: We use a series of digital image processing techniques to measure the width of central balding area of FPHL. A total of 184 photos were collected form 33 Chinese women with FPHL (stages I-2 to II-2 on the Savin scale). Each photograph underwent standardized exposure correction. The balding areas were detected through this computer system and then transformed into an equivalent ellipse by principal component analysis. The width of ellipse [balding width (BW)] was measured. Spearman's rank correlation was used to detect the correlation between our measurements and clinical staging.
Results: Exposure correction resulted in a 16.97% ($|BW_{corrected} - BW_{original}|/BW_{corrected}$) difference in BW. The average BW was 54.98 mm in all patients, 25.79 mm in type I-2 patients, 37.41 mm in I-3, 54.08 mm in I-4, 72.10 mm in II-1, and 85.53 mm in II-2. The values of BW were correlated with Savin scale stages clinically ($r_{BW} = 0.967$), which was significant statistically ($p < 0.05$).
Conclusion: A computer-aided imaging system could be a useful tool to assist physicians to evaluate the balding area more precisely for clinical staging in FPHL. The BW instead of the balding area is simple to use clinically to represent the severity of FPHL.

Introduction

Female pattern hair loss (FPHL) is a common hair loss disease in women.[1] Typical features of FPHL are miniaturizations of hair follicles in the central scalp (vertex, mid, and frontal), bitemporal, and parietal regions.[2] Conventional balding scales such as the Ludwig and Savin scales are used widely for grading FPHL.[3–7] However, estimation by visual inspection may cause variation among different physicians in terms of assessment of hair loss and subsequent treatment response. For this reason, we propose a computer-aided imaging system (CAIS) to help physicians in clinical staging of FPHL. The CAIS includes fixed camera setting, exposure correction of images, Chan and Vese level-set scheme, and principal component analysis. Using this system, balding width (BW) was measured to represent the severity of FPHL, which can be served as an assistant tool for common grading system used clinically and for follow-up assessment of treatment response.

Methods

The image analysis was performed on 184 photos collected from 33 Chinese women, aged 20–50 years, with FPHL (stages I-2 to II-2 on the Savin scale). Patients with gray hair or those using a hair dye

Conflicts of interest: The authors declare that they have no financial or nonfinancial conflicts of interest related to the subject matter or materials discussed in this article.

* Corresponding author. Institute of Biomedical Engineering, National Taiwan University, Number 1, Section 4, Roosevelt Road, Taipei, Taiwan.
E-mail address: chung@ntu.edu.tw (C.-M. Chen).

http://dx.doi.org/10.1016/j.dsi.2015.01.002

were excluded from this study. Prior to taking photos, each patient was asked to part her hair centrally. Photos with a 45° frontal view were taken by Nikon D700 (Nikon Corporation, Tokyo, Japan) with the following default settings: aperture F-22, shutter speed 1/6400 seconds, ISO 200, automatic white balance, 300 dot-per-inch, and a resolution of 3008 × 2000. The camera flashlight was charged fully prior to taking each photo. Two metal mounts were designed to fix the positions of both camera and participant's forehead, for exposure collection and to maintain consistent position.

Hermite spline, a grayscale transformation scheme and a common strategy for exposure correction, was used in this study.[8] This was achieved by calibrating each photo to a fixed object, which in our study was the metal piece of the forehead mount on the photo device.

For exposure correction, the original images with 8-bit grayscale were changed into intensity images ranged from 0 (black) and 1 (white). In each image, pixels exhibiting the metal piece were calculated with mean value of intensity (M_n, $n = 1, 2, 3, \ldots 184$). The average of all M_n values was set as the threshold (M_t) for the calibration. To achieve interpolation of the Hermite spline, the transform function was defined as follows:

$$p(t) = h_{00}(t)p_0 + h_{10}(t)m_0 + h_{01}(t)p_1 + h_{11}(t)m_1 \quad (1)$$

$$h_{00} = 2t^3 - 3t^2 + 1 \quad (2)$$

$$h_{10} = t^3 - 2t^2 + t \quad (3)$$

$$h_{01} = -2t^3 + 3t^2 \quad (4)$$

$$h_{11} = t^3 - t^2 \quad (5)$$

where h_{00}, h_{10}, h_{01}, and h_{11} are Hermite basis functions and $t \in [0, 1]$; p_0 is the starting point ($t = 0$) with tangent m_0, and p_1 the ending point ($t = 1$) with tangent m_1. Image can be gradually corrected by adapting different tangents at the starting and ending points. Once M_t and an optimized M_n of the corrected image became equal, exposure correction was completed (Figure 1). In this study, the default setup of M_t is 0.07.

After exposure correction, brightness on all images was equal, and the region of balding area (sparse hair) was delineated automatically by the Chan and Vese level-set scheme. The energy function of the level-set scheme was defined as follows:

$$F_1F1 = \int_{\text{inside}(C)} |I(x,y) - m_1m1|^2 \mathrm{d}x\mathrm{d}y \quad (6)$$

$$F_2F2 = \int_{\text{outside}(C)} |I(x,y) - m_2m2|^2 \mathrm{d}x\mathrm{d}y \quad (7)$$

$$E(C, m_1m1, m_2m2) = u^*\text{length}(C) + v^*\text{area}(\text{inside}(C)) + \lambda_1{}^*F_1F1 + \lambda_2{}^*F_2F2 \quad (8)$$

In these equations, $I(x, y)$ was the grayscale of pixel (x, y). C represents the evolving contour of the balding area and length (C) its circumference. F_1 and F_2 were used to validate the homogeneity of pixels within and outside C, where m_1 and m_2 were the mean values of the grayscale of pixels within and outside C, respectively. The area inside the contour, area [inside (C)], was equal to the balding area; u, v, λ_1, and λ_2 were weighting factors. Minimization of the energy function E resulted in an update of C. Once the minimal E was computed, an optimal C was determined.[9,10] In our study, the default setup parameters for the weighting factors were as follows: $u = 0$, $v = 0.01$, $\lambda_1 = 1$, and $\lambda_2 = 1$.

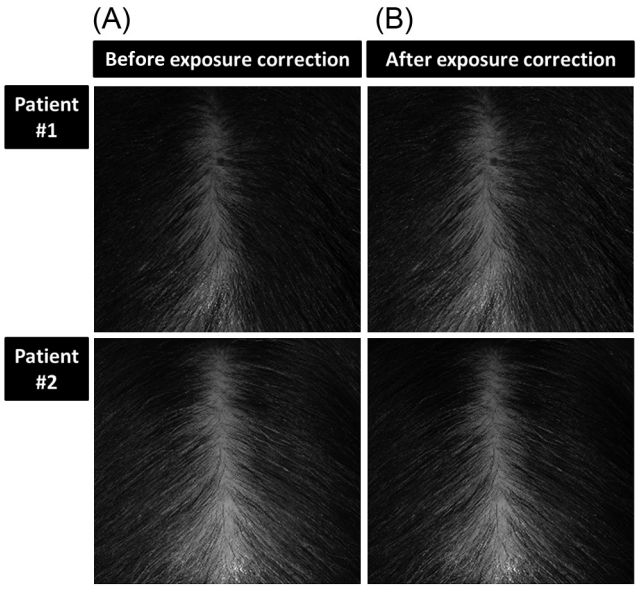

Figure 1 Images of Patient #1 and Patient #2 with the same clinical grading (Savin scale I-4). (A) Original images. (B) Images after exposure correction.

The irregular contour of the balding area was depicted by the complex mathematical formula described above. The irregular contour was then transformed into an equivalent ellipse using principal component analysis. Principal component analysis was performed by measuring the covariance of pixels, as follows:

$$\text{covariance matrix} = \begin{bmatrix} \text{cov}(x,x) & \text{cov}(x,y) \\ \text{cov}(y,x) & \text{cov}(y,y) \end{bmatrix} \quad (9)$$

$$\text{cov}(x,x) = \frac{1}{n-1} \times \sum_{p=1}^{n} (X_p - \overline{X}) \times (X_p - \overline{X}) \quad (10)$$

$$\text{cov}(y,y) = \frac{1}{n-1} \times \sum_{p=1}^{n} (Y_p - \overline{Y}) \times (Y_p - \overline{Y}) \quad (11)$$

$$\text{cov}(x,y) = \text{cov}(y,x) = \frac{1}{n-1} \times \sum_{p=1}^{n} (X_p - \overline{X}) \times (Y_p - \overline{Y}) \quad (12)$$

The center of the balding area $(\overline{X}, \overline{Y})$, also the center of an equivalent ellipse, was calculated by averaging coordinates of n-pixels (x, y) in the area. Both eigenvalues and eigenvectors of the covariance matrix were computed. Once eigenvectors are found, they were ordered according to eigenvalues, from highest to lowest, denoting components in order of significance. Using these values and unit vectors, orientation of the equivalent ellipse can be determined. Then, the width of the ellipse was measured. The details of principal component analysis have been described in Jolliffe's textbook.[11] For convenience in clinical use, the width of the ellipse was chosen to represent the balding area and it was measured (Figure 2).

Spearman's rank correlation was performed to detect the correlation between our measurements and clinical staging for all patients ($n = 33$).

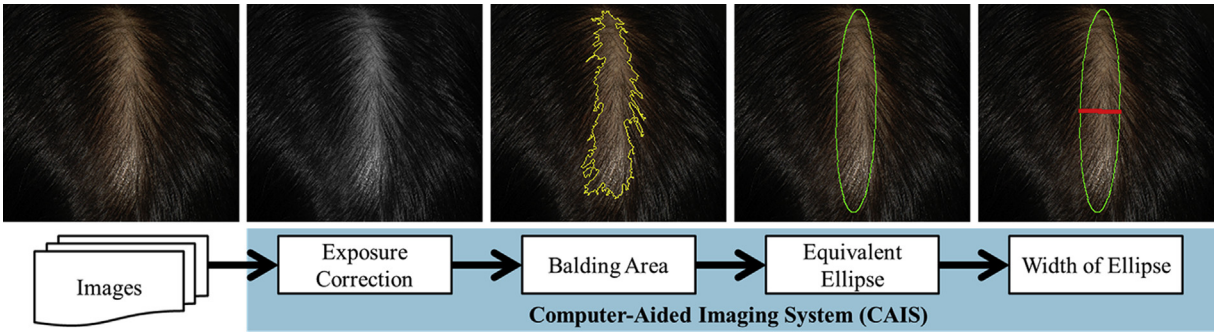

Figure 2 Processing of computer-aided imaging system. Balding area (yellow line), equivalent ellipse (green line), and balding width (width of ellipse, red line) are demonstrated.

Results

The efficacy of exposure correction was validated through comparison of photos prior to and after processing (Figure 3). Exposure correction resulted in a 16.97% ($|BW_{corrected} - BW_{original}|/BW_{corrected}$) difference in BW. The average BW was 54.98 mm in all patients, 25.79 mm in type I-2 patients, 37.41 mm in I-3, 54.08 mm in I-4, 72.10 mm in II-1, and 85.53 mm in II-2 (Table 1). The values of BW were correlated with Savin scale stages clinically ($r_{BW} = 0.967$), which was significant statistically ($p < 0.05$). Figure 4 demonstrates the balding area (green contour) and ellipse (red contour) for FPHL patients at different Savin scale stages.

Discussion

FPHL is a common disease in females with hair loss.[1] Clinical staging for FPHL using the Ludwig and Savin scales is based on visual inspection, which may cause much variation in disease assessment and treatment among physicians. For this reason, we proposed a CAIS to measure BW to help physicians in clinical staging of FPHL. Prior to measurement, exposure correction was performed by Hermite spline. This is the first attempt to be applied in clinical use, which can correct the possible artifacts in biased photos. Exposure correction and its compensation for biased photos under different photographic conditions can be very useful for more precise evaluation, to achieve better consistency and reproducibility. This was validated through comparison of photos prior to and after processing. In this study, exposure correction resulted in a 16.97% difference in BW.

Table 1 demonstrates the correlation between Savin scale grading and values of BW. The values of BW were correlated with Savin scales clinically ($r_{BW} = 0.967$). The values between different Savin scales were significant statistically ($p < 0.05$). From results of our study, quantitation of BW may be used to evaluate balding

Table 1 Correlation between computed BW and clinical hair loss severity by Savin Scale.

Grading (Savin)	Patients	Photos	BW (mm)
			Mean ± SD
I-2	9	47	25.79 ± 2.42
I-3	9	52	37.41 ± 6.23
I-4	9	55	54.08 ± 7.00
II-1	3	16	72.10 ± 6.25
II-2	3	14	85.53 ± 3.98

BW = balding width.

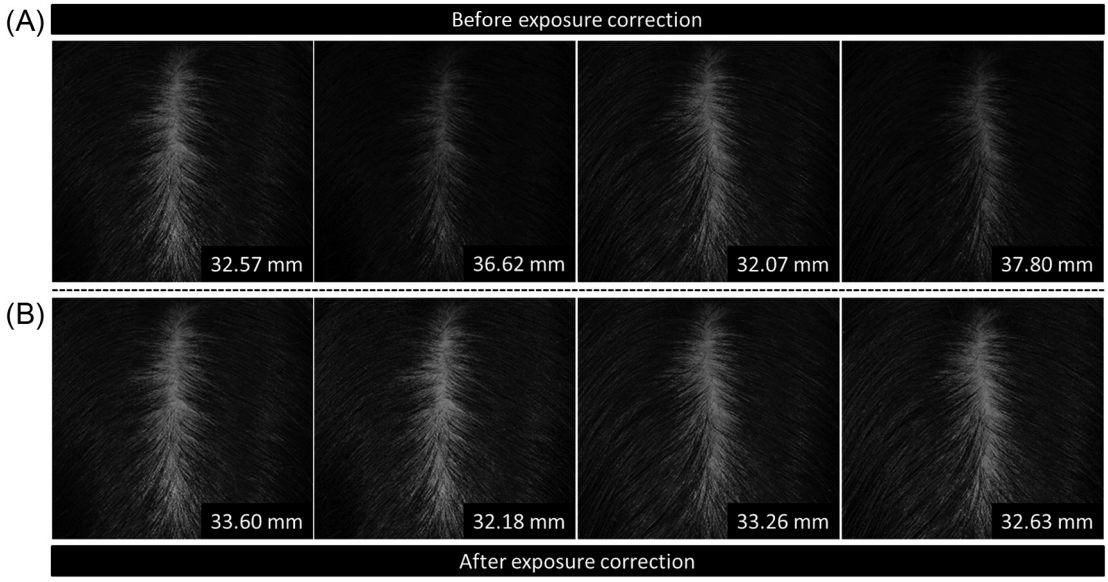

Figure 3 Serial photos of each FPHL patient were (A) taken and (B) corrected prior to calculating the baldness width. An overestimation of baldness width occurs in images with a poor image contrast.

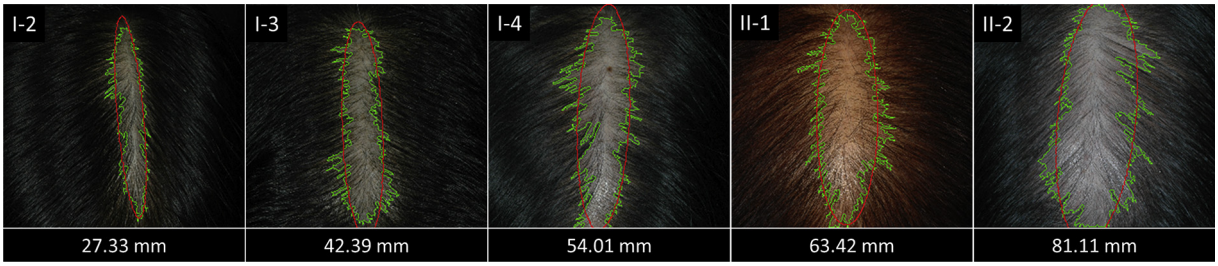

Figure 4 After exposure correction, the bald area (green contour) and bald ellipse (red contour) were calculated from photos of FPHL patients at different Savin scale stages.

status and monitor the progression of hair loss in patients with FPHL. The reason for measuring BW is that it was easy be apply in clinical use. Physicians may just measure the width of the central balding area for objective evaluation of patients with FPHL and to monitor progression of hair loss and treatment response by repeated measurement in their offices. This may be further assisted by more data collected from future studies on the range of BW in each scales of Savin or Ludwig.

From this preliminary study, CAIS has been proved to be useful for measurement of BW from photos of patients with FPHL. This technique is still under development and needs to be improved prior to being widely used clinically. First, the system has to accommodate all camera settings and be applied to patients of different races and with different hair colors. We hope that this technique can be refined and accomplished in the near future. Further clinical studies will also be conducted.

In conclusion, BW measured by a CAIS was useful for clinical assessment of patients with FPHL and even for quantitative follicular unit transplantation surgery.[12] The results from the present study are encouraging for future research.

References

1. Olsen EA. Female pattern hair loss. *J Am Acad Dermatol* 2001;**45**(3 Suppl.): S70–80.
2. Olsen EA. Current and novel methods for assessing efficacy of hair growth promoters in pattern hair loss. *J Am Acad Dermatol* 2003;**48**:253–62.
3. Ludwig E. Classification of the types of androgenetic alopecia (common baldness) occurring in the female sex. *Br J Dermatol* 1977;**97**:247–54.
4. Savin R. A method for visually describing and quantitating hair loss in male pattern baldness. *J Invest Dermatol* 1992;**98**:604 [Abstract].
5. Olsen EA, Messenger AG, Shapiro J, et al. Evaluation and treatment of male and female pattern hair loss. *J Am Acad Dermatol* 2005;**52**:301–11.
6. Shapiro J. Clinical practice. Hair loss in women. *N Engl J Med* 2007;**357**: 1620–30.
7. Whitting DA. *Hair growth and disorders*. Berlin, Heidelberg: Springer; 2008.
8. Gonzalez RC, Woods RE. *Digital image processing*. 3rd ed. Upper Saddle River: Prentice Hall; 2007.
9. Chan TF, Vese LA. Active contours without edges. *IEEE Trans Image Process* 2001;**10**:266–77.
10. Sethian JA. *Level set methods and fast marching methods: evolving interfaces in computational geometry, fluid mechanics, computer vision, and materials science*. 2nd ed. Cambridge: Cambridge University Press; 1999.
11. Jolliffe IT. *Principal component analysis*. 2nd ed. New York: Springer; 2002.
12. Tsai RY, Lee SH, Chan HL. The distribution of follicular units in the Chinese scalp: implications for reconstruction of natural-appearing hairlines in Orientals. *Dermatol Surg* 2002;**28**:500–3.